Natural Resources for Human Health
eISSN: 2583-1194

Original Research

Received 05 July 2026
Revised 11 Aug 2026
Accepted 25 Aug 2026

Natural Resources for Human Health 2026, Vol. 6 (19s): 960–973

KEYWORDS:
Hypericum perforatum; Silver nanoparticles; Antibacterial activity; Wound healing; topical gel; Infrared thermography.

Phyto-Synthesized Silver Nanoparticles: A Hypericum perforatum-Mediated Approach for Topical Wound Healing Gels

Abdulrhman A. Ismael[1], Maimonah Q. Yahya[1], Zena Sattam Hamad[2]

[1]Department of Clinical Laboratory Science, College of Pharmacy, Mosul University, Mosul, Iraq
[2]Department of Pharmacology and Toxicology, Mosul , University, Mosul,Iraq

ABSTRACT: The current study was aimed at the comparative preparation of silver nanoparticles (AgNPs) using chemical and green methods with the ethanolic extract of Hypericum perforatum and inclusion in a topical gel (Carbopol) to assess their efficiency in the treatment of infected wounds. The methodology consisted of: characterization of the particles by using (UV-Vis, FTIR, SEM, DLS), evaluation of the antibacterial activity, physical properties of the gel and its dermal safety, as well as biological evaluation (in vivo) in a model of albino rats with linear wounds infected with Staphylococcus aureus bacteria, using morphological measurements, infrared thermography and bacterial cultures. The results showed the superiority of the green synthesis nanoparticles (P. NPs) in antibacterial activity as the lowest minimum inhibitory concentration (MIC) and minimum bactericidal concentration (MBC) values were recorded compared to the chemical nanoparticles and the crude extract. In animal studies, the gel group containing green nanoparticles showed the highest wound closure rate (91.80%), no detectable bacterial growth by day 6, and thermal convergence (ΔT = +0.10°C). The results of this study showed that the green synthesis of silver nanoparticles by H. perforatum showed promising antibacterial and wound healing activity with short term dermal tolerability.

1. INTRODUCTION

Infected skin wounds, especially chronic or severe ones, constitute a serious clinical problem in modern health care associated with high morbidity and mortality rates as well as with significant treatment costs [1]. This problem is made worse by the global phenomenon of antibiotic resistance, where infectious bacteria like *Staphylococcus aureus* and *Pseudomonas aeruginosa* have devised sophisticated mechanisms to escape conventional therapy and build resistant biofilms [2]. Therefore, there is an urgent need in the scientific and medical communities for the search for new and effective therapeutic alternatives that can simultaneously fight microbes and promote wound healing [3].

In this aspect, the medicinal plants have become a promising source of the bioactive compounds with antimicrobial, anti-inflammatory and tissue-regenerative properties [4]. One of the most important traditional plants used for wounds and burns is St. John's wort (*Hypericum perforatum*). Recent studies have shown that its extracts contain high levels of phenolic compounds, flavonoids and naphthodianthrones that are essential in accelerating wound healing and inhibiting bacterial growth [5]. Studies have shown that ethanolic extracts of this plant are very effective in shrinking wound size and stimulating the formation of new blood vessels in animal models [6].

On the other hand, the field of biomedicine has been revolutionized by nanotechnology. Silver nanoparticles (AgNPs), in particular, have gained a lot of attention because of their broad-spectrum antimicrobial activity, ability to penetrate bacterial cell membranes, and multiple mechanisms of action that reduce the likelihood of bacteria developing resistance [7,8].

However, the conventional chemical synthesis methods for silver nanoparticles employ toxic reducing and stabilizing agents, raising concerns regarding their cytotoxicity and biocompatibility, particularly in topical dermatological applications [9]. To overcome these barriers, the concept of "green synthesis" was developed as an environmentally friendly and sustainable approach, utilizing plant extracts as natural reducing and stabilizing agents rather than toxic chemicals [10]. Secondary plant metabolites like phenols and flavonoids present in *Hypericum perforatum* act as a natural coating around the nanoparticles which improves their biostable properties and may provide an additional effect that enhances their antibacterial efficacy as compared to chemically synthesized particles or crude plant extracts [11].

The development of topical drug delivery systems is important for improving clinical efficacy of these nanoparticles. Topical formulations often use polymer-based gels like carbomer (Carbopol) because of their capacity to maintain an ideal moist environment in the wound, allow drug diffusion, minimize evaporative fluid loss and possess physicochemical properties compatible with the skin pH [12]. Moreover, infrared thermography has proven to be a valuable non-invasive diagnostic tool for monitoring wound healing dynamics, as it reflects changes in local perfusion, metabolism and inflammation by measuring the temperature differences between the wound and healthy skin [13].

Based on the above, the aim of this study is the chemical synthesis of silver nanoparticles with ethanolic extract of *Hypericum perforatum*, and their characterization with different techniques (UV-Vis, FTIR, SEM, DLS). The study also focuses on the development of these nanoparticles in Carbopol based topical gel and evaluation of their antibacterial activity, physical characteristics and skin safety. Finally, the efficacy of these gels in the treatment of *S. aureus* infected linear wounds on an albino rat model is evaluated using thermography, morphological measurements and bacterial cultures as comprehensive evaluation tools.

2. MATERIALS AND METHODS

2.1 Preparation of the Plant Extract and Chemical Analysis:

The aerial parts of *Hypericum perforatum* were purchased from a local market in Mosul, Iraq, and their botanical identity was verified by Dr. Mai Taha in the Department of Biology, College of Science, University of Mosul. The plant parts were thoroughly washed with distilled water, dried in the shade, and ground using a 100-mesh sieve. Twenty grams of the powder were extracted using absolute ethanol at a constant ratio of 1:10 (w/v) and then treated with an ultrasonic bath LUC-405 (Lab Teck, Korea) for one hour [14]. The solution was filtered, and the solvent was removed under vacuum using a rotary evaporator (Lab tech EV400H, China) at 40°C. The dry extract was then weighed and stored in a tightly sealed container at 4°C. A qualitative phytochemical screening was performed using a 1% aqueous suspension of the ethanolic extract to detect phenols (ferric chloride test), flavonoids (alkali reagent test), tannins (lead acetate test), alkaloids (Mayer's test), quinones (concentrated sulfuric acid test), carbohydrates (Molisch's test), steroids (Salkowski test), and saponins (foam test). Coumarins were also tested using sodium hydroxide and UV light [15-18].

2.2 Preparation of chemical and green silver nanoparticles (AgNPs):

The nanoparticles were chemically prepared using polyvinylpyrrolidone (PVP) as a stabilizing agent and sodium borohydride ($NaBH_4$) as a reducing agent. 849.35 mg of silver nitrate was dissolved in 500 mL of distilled water to prepare a 0.01 M solution. 1.0 g of PVP was added, and the mixture was maintained in an ultrasonic bath at 30 °C with pH adjusted to 7.0. while adding a 48 mL of fresh $NaBH_4$ solution (0.01 M) dropwise at a rate of 1 mL/min under continuous sonication for 50 minutes [19]. In contrast, plant-mediated nanoparticles (green method) were prepared by mixing 100 mg of plant extract and 100 mg of PVP in a flask, followed by the addition of 100 mL of silver nitrate solution (5 mM) dropwise at a rate of 1 mL/min. The mixture was subjected to sonication at 50 °C for 45 minutes and then both nanoparticle suspensions were left in the dark for 48 hrs to complete dispersion and reduction. The nanoparticle suspensions were centrifuged at 13,000 rpm for 45 minutes, washed three times with distilled water, and then dried in a hot air oven at 40 °C for 12 hrs [20].

2.3 Nanoparticle Characterization Analysis:

Samples were analyzed using Fourier transform infrared spectroscopy (Shimadzu IRXross FTIR spectrophotometer, Japan) to identify functional groups [20]. UV-Vis spectra, Thermo Scientific GENESYS 180, USA) were also recorded over wavelength of 300–700 nm to detect surface plasmon resonance [21]. Surface morphology and aggregation were studied using scanning electron microscopy (Ziess EVO 10 SEM, Germany) after coating the samples with a 1 nm thick gold layer [22].

Hydrodynamic diameter and polydispersity index (PDI) were measured using dynamic light scattering (DLS) with a Litesizer (Anton paar, Austria) after a 1:10 dilution of the samples [23].

2.4 Antibacterial activity evaluation:

The plant extract, chemically synthesized silver nanoparticles, and plant-mediated silver nanoparticles were tested against Gram-positive (S. *aureus, S. epidermidis, E. faecalis*) and Gram-negative (P. *aeruginosa, E. coli, K. pneumoniae, A. baumannii)* bacteria using well diffusion method on Mueller-Hinton agar with 8 mm well diameter, with gentamicin disk (10 µg) as the positive control and distilled water and 1% DMSO as the negative controls [24]. The minimum inhibitory concentration (MIC) was determined by microdilution method using 96 well plate with blank for each dilution, and bacterial growth was measured at 610 nm. For determination of the minimum bactericidal concentration (MBC), 0.1 mL was collected from wells showing no detectable bacterial growth and from the next higher concentration, then inoculated onto nutrient agar and incubated for 24 h. The MBC was defined as the lowest concentration showing no visible bacterial growth after incubation [25].

2.5 Preparation and evaluation of Carbopol gel and irritation testing:

Four formulations of Carbopol 934 gel were prepared using 0.0625 g in 25 mL of distilled water. These formulations included: a blank gel, a plant extract gel (2.5% w/v), a green nanogel (0.025% w/v), and a chemical nanogel (0.032% w/v). Three to four drops of triethanolamine were then added to adjust PH [26]. The gels were evaluated for homogeneity, coarseness, pH, spreadability and viscosity using a Drawell (NDJ-8S, china) at 25°C and 30 rpm [27-29]. Skin irritation testing was also performed on three healthy albino rats by applying the preparations to shaved areas of the back and comparing them to control areas, monitoring for erythema or edema after 24, 48, and 72 hrs [30].

2.6 Animal Model and Wound Healing Evaluation:

Thirty five male albino rats (204–288 g) were used in this study from the Animal House, College of Veterinary Medicine, University of Mosul (approval no. UM.VET.2026.005). The animals were acclimatized for 7 days. The rats were anesthetized with ketamine (90 mg/kg) and xylazine (10 mg/kg), and a superficial linear wound (30 ± 3 mm) was created and infected with 0.1 mL of 0.5 McFarland *S. aureus* culture solution (1.5×10^8 CFU/mL) from Groups 2 to 7 [31]. The experimental animals were randomly allocated into seven groups (n = 5 per group): Group 1 (uninfected, untreated control), Group 2 (infected, untreated control), Group 3 (infected + plain gel), Group 4 (infected + chemical nanoparticles), Group 5 (infected + plant extract), Group 6 (infected + green synthesized nanoparticles), and Group 7 (infected + 0.1% clindamycin as a standard positive control. The wound was treated topically with 0.5 g of the assigned gel daily for 7 days, after 24 hours of wound induction. Woundhealing was assessed by digital photography, wound dimension measurement and infrared thermography (FLIR ONE camera at 30 cm, 0.95 emissivity, room temperature 27°C) to determine the temperature difference on days 1, 3, 5, 7 (ΔT = wound temperature – adjacent healthy skin temperature) [32]. Bacterial cultures were obtained on mannitol salt-agar daily. Wound closure percentage was calculated

2.7 Statistical analysis

statistical analyses were performed using GraphPad Prism 9.0 (Friedman's test) .The values were expressed as means ± standard deviation (SD), The experimental results were analyzed by running a oneway ANOVA test followed by the Tukey's for multiple comparisons, $P<0.05$ was considered statistically significant)

3. RESULTS

3.1 Extraction Yield, Phytochemistry, and Particle Characterization:

The absolute ethanol extraction yield was 3.68% (0.736 g from 20 g powder), yielding a viscous, dark green extract. Phytochemistry showed strong positive results for phenols and flavonoids, moderate results for tannins and alkaloids, and weak results for carbohydrates, quinones, steroids, and saponins, while coumarins were not detected as shown in table 1and figure 1.

Natural Resources for Human Health
eISSN: 2583-1194

Table 1. Qualitative phytochemical screening of *Hypericum perforatum* ethanolic extract

Phytochemical constituent	Test name	Result
Phenols	Ferric chloride test	+++
Flavonoids	Alkaline reagent test	+++
Tannins	Lead acetate test	++
Alkaloids	Mayer's test	++
Quinones	Concentrated H_2SO_4 test	+
Steroids	Salkowski test	+
Carbohydrates	Molisch's Test	+
Saponins	Frothing test	+
Coumarins	NaOH/ UV test	-

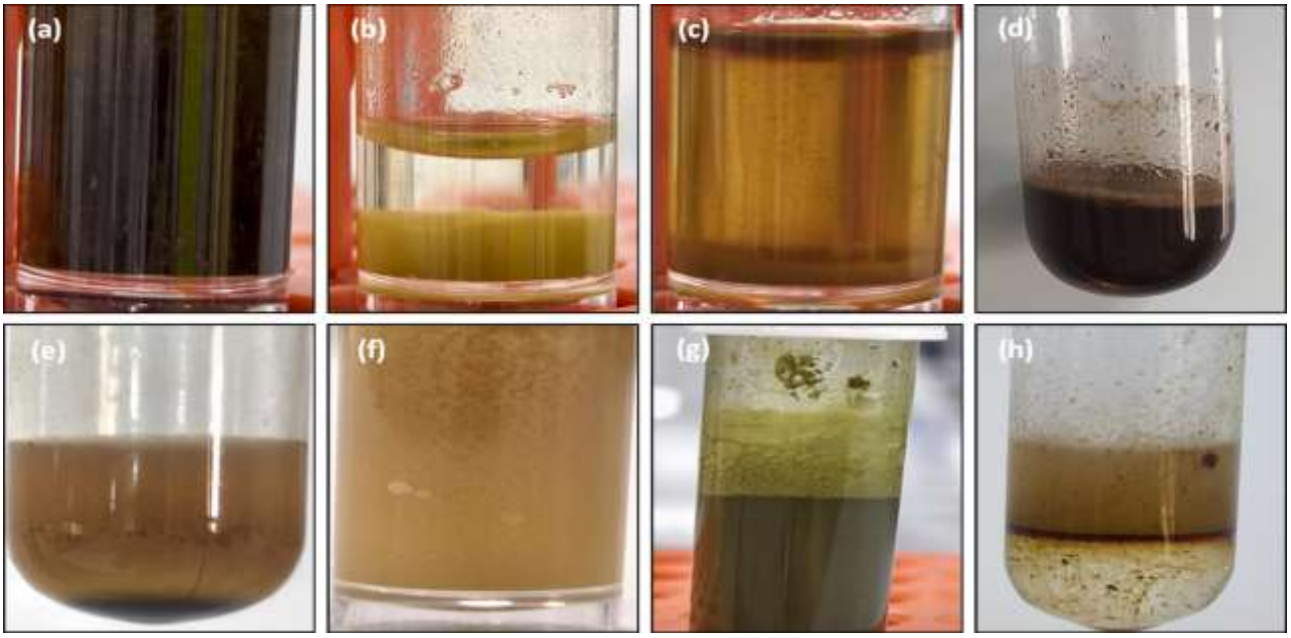


Figure 1. Qualitative phytochemical screening of the ethanolic extract of *Hypericum perforatum*: A, phenols; B, tannins; C, flavonoids; D, quinones; E, carbohydrates; F, alkaloids; G, saponins; and H, steroids.

UV-Vis spectroscopy confirmed particle formation by the appearance of a surface plasmon resonance peak at 425 nm for chemical nanoparticles and 440 nm for plant nanoparticles. FTIR spectroscopy confirmed the interaction of plant functional groups (such as O-H at 3304 cm^{-1} and C=O at 1608 cm^{-1}) in the reduction and stabilization of plant particles as presented in figure 2.

Natural Resources for Human Health
eISSN: 2583-1194

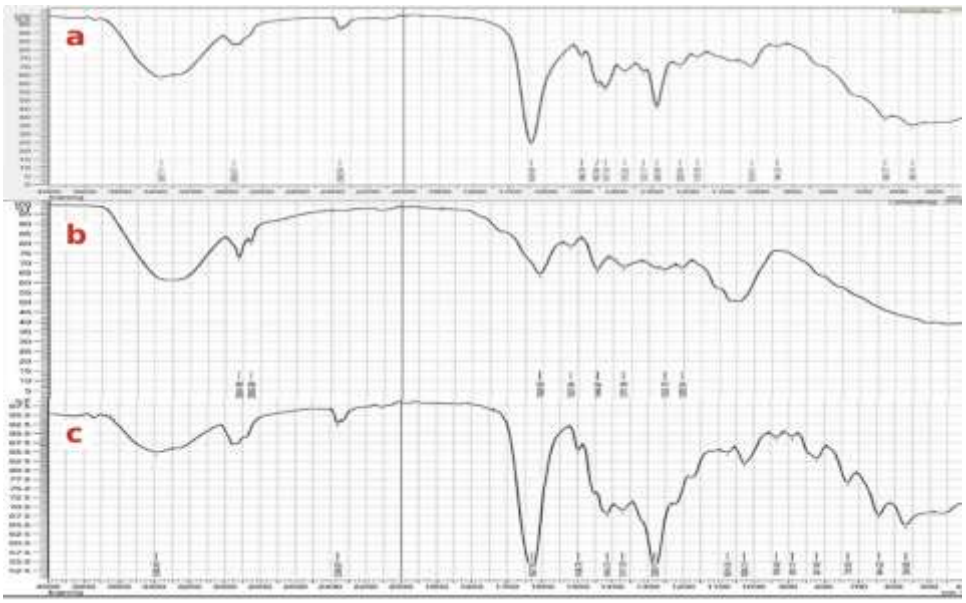


Figure 2. FTIR spectra of: A, chemically synthesized AgNPs; B, *Hypericum perforatum* extract; and C, plant-mediated AgNPs.

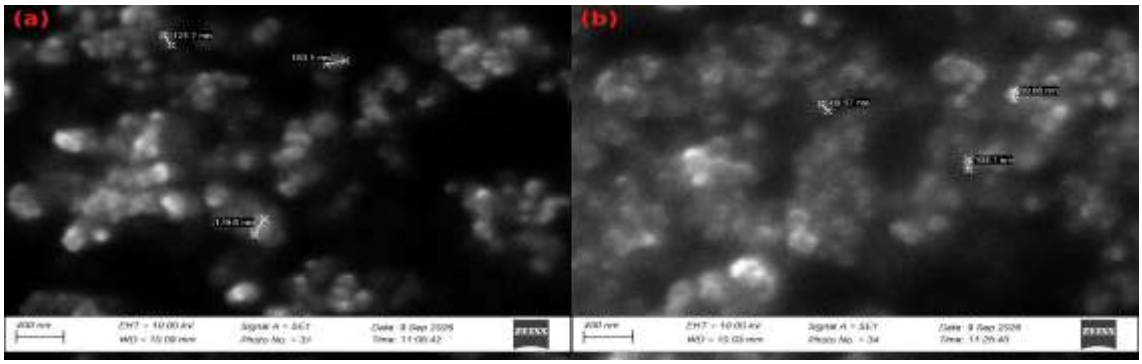


Figure 3: SEM image of (a) P. NPs and (b) AgNPs. at 400nm.

Electron microscopy (SEM) image revealed that chemical silver nanoparticles and plant nanoparticles were single pellets with some aggregation and their diameter ranging from 89.57 to 103.1 and 121.7 to 179.6 nm, respictively. Thes findings confirm they fail in nanometeric range as shown in figure 3.

DLS analysis revealed an average hydrodynamic size of 57.67 nm (PDI 0.437) for the chemical nanoparticles and 114.33 nm (PDI 0.409) for the plant nanoparticles, indicating a broad size distribution for both as indicated in figure 4.

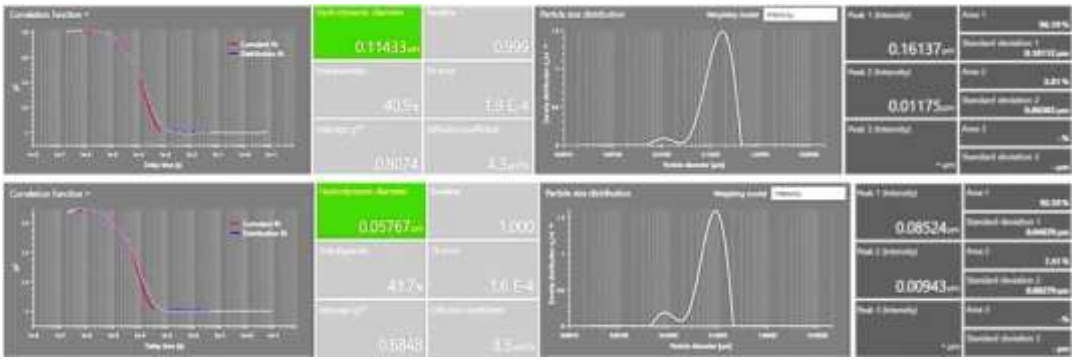


Figure 4. Intensity-weighted particle-size distributions of: A, plant-mediated AgNPs; and B, chemically synthesizedAgNPs, obtained using the Litesizer software.

Natural Resources for Human Health
eISSN: 2583-1194

3.2 Antibacterial Activity:

Preliminary screening showed that the crude plant extract was effective only against *S. aureus, S. epidermidis, and P. aeruginosa*, while other bacteria showed no inhibition as shown in table 2. At a concentration of 12.5 mg/ml, plant nanoparticles (P.NPs) exhibited the largest inhibition zones (38 mm against *P. aeruginosa* and 36 mm against both *Staphylococcus aureus* and *Staphylococcus epidermidis)*, followed by chemical nanoparticles (30 mm and 28 mm, respectively), while the plant extract showed inhibition zones of 11.5, 15, and 13 mm as shown in table 2.

Table 2. Comparative agar well-diffusion results for the three test preparations

Bacterial isolate	Preparation	Test concentration (mg/mL) Zone of inhibition: mean ± SD (mm)									Controls	
		100	50	25	12.5	6.25	3.125	1.6	0.78	0.39	DW/1% DMSO	GEN 10 µg
S. aureus	P.EX	21.0±0.2	20.5±0.2	19.0±0.5	15.0±0.3	14.0±0.3	11.0±0.2	0.0±0.0	0.0±0.0	0.0±0.0	0.0±0.0	20.0±0.0
S. aureus	P.NPs	42.5±0.5	40.0±0.5	38.0±0.4	36.0±0.2	35.5±0.2	35.0±0.4	30.0±0.5	23.0±0.5	21.0±0.2		
S. aureus	AgNPs	40.0±0.5	36.0±0.5	33.5±0.5	28.0±0.6	27.0±0.4	26.0±0.3	24.0±0.2	20.0±0.2	19.0±0.2		
P. aeruginosa	P.EX	24.0±0.1	22.5±0.5	16.5±0.4	11.5±0.5	10.5±0.3	0.0±0.0	0.0±0.0	0.0±0.0	0.0±0.0	0.0±0.0	22.0±0.0
P. aeruginosa	P.NPs	45.0±0.5	43.0±0.5	40.0±0.5	38.0±0.4	37.0±0.6	36.0±0.2	33.0±0.3	24.0±0.2	22.0±0.4		
P. aeruginosa	AgNPs	42.0±0.5	38.0±0.5	34.0±0.5	30.0±0.6	28.0±0.5	26.0±0.3	24.0±0.4	19.0±0.3	18.0±0.4		
S. epidermidis	P.EX	20.5±0.3	19.5±0.3	17.5±0.5	13.0±0.6	11.0±0.3	0.0±0.0	0.0±0.0	0.0±0.0	0.0±0.0	0.0±0.0	20.0±0.0
S. epidermidis	P.NPs	42.0±0.4	40.0±0.4	38.0±0.3	36.0±0.4	30.0±0.4	25.0±0.4	23.0±0.1	20.0±0.4	17.0±0.2		
S. epidermidis	AgNPs	40.5±0.3	36.0±0.4	33.0±0.3	28.0±0.4	27.0±0.5	26.0±0.4	21.0±0.5	17.0±0.3	15.0±0.2		

Abbreviations: ZOI, zone of inhibition; SD, standard deviation; P.EX, crude plant extract; P.NPs, plant-mediated silver nanoparticles; AgNPs, chemically synthesized silver nanoparticles; DW, distilled water; DMSO, dimethyl sulfoxide; GEN, gentamicin; mg/mL, milligram per millilitre; mm, millimetre

Microdilution testing determined that plant nanoparticles achieved the lowest MIC and MBC values (0.02 mg/ml) against *Staphylococcus aureus,* outperforming chemical nanoparticles (0.025 mg/ml). The plant extract required much higher concentrations against *S. aureus,* with an MIC of 1.562 mg/ml and an MBC of 3.125 mg/ml as summarized in table 3. As for *P. aeruginosa*, although large inhibition zones appeared in the diffusion assay, it registered very high values in MIC and MBC

200 mg/ml for plant extract, whereas P. NPs and AgNPs showed lower values of 0.19 and 0.2 mg/mL, respectively. These findings indicate higher tolerance of *P. aeruginosa* compared to *S. aureus* as demonstrated in figures 5.

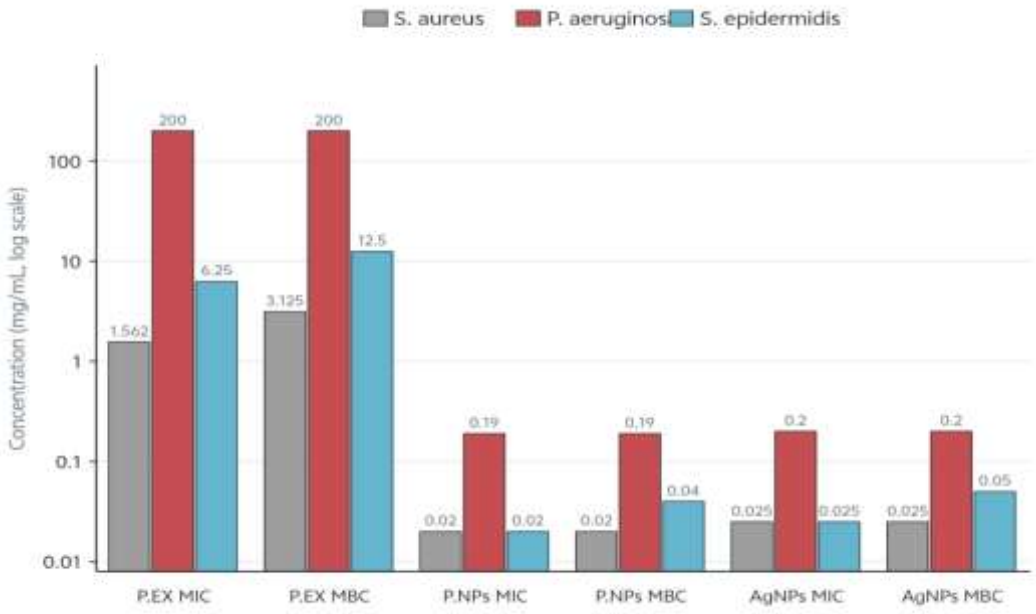


Figure 5. Comparative MIC and MBC values of the three tested preparations against the responsive bacterial isolates.

3.3 Gel Properties and Irritation Test:

All four gel formulations exhibited complete homogeneity, a smooth texture, and were free from roughness or lumps (although the plant extract gel appeared turbid due to the plant dispersants). The pH ranged from 5.68 to 6.28, which are mildly acidic to neutral values suitable for the skin application. Viscosity ranged from 20,461 to 21,360 cP as shown in table 4. The ZOI was 14 mm for Clindamycin and P. EX gel, 21 for P.NPs gel and 14.5 mm for AgNPs gel. Irritation testing showed no observable erythema, edema, blistering, or local skin reactions with any formulation observed during the monitoring period (24, 48, and 72 hrs).

Table 4. Physicochemical characteristics of the prepared gel formulations.

Formulation	Appearance	Homogeneity	Grittiness	pH	Spreadability (cm)	Viscosity (cP)
Plain Carbopol gel	Clear	Homogeneous	Smooth	5.74±0.04	5.4±0.082	21,360±98
Plant-extract gel	Turbid	Homogeneous	Smooth	6.28±0.05	5.35±0.23	20,461±93
P.Nps gel	Clear	Homogeneous	Smooth	5.69±0.03	5.37±0.05	21,310±87
AgNPs gel	Clear	Homogeneous	Smooth	5.68±0.03	5.42±0.09	21,260±95

3.4 In vivo wound healing and thermal imaging:

On day 3, wound closure ranged from 38.94% (untreated infected group) to 52.73% (untreated uninfected group). However, the differences between the treated groups were not statistically significant (P>0.05). On day 5, closure increased significantly, with the plant nanoparticle group showing the highest closure (77.48%), followed by the chemical nanoparticle group(75.51%), again without statistically significant differences (P>0.05). On day 7, the plant nanoparticle group achieved the highest terminal closure (91.80%), followed by the clindamycin group (90.68%), the chemical nanoparticle group (90.60%), and the plant extract group (89.53%) as depicted in figure 6.

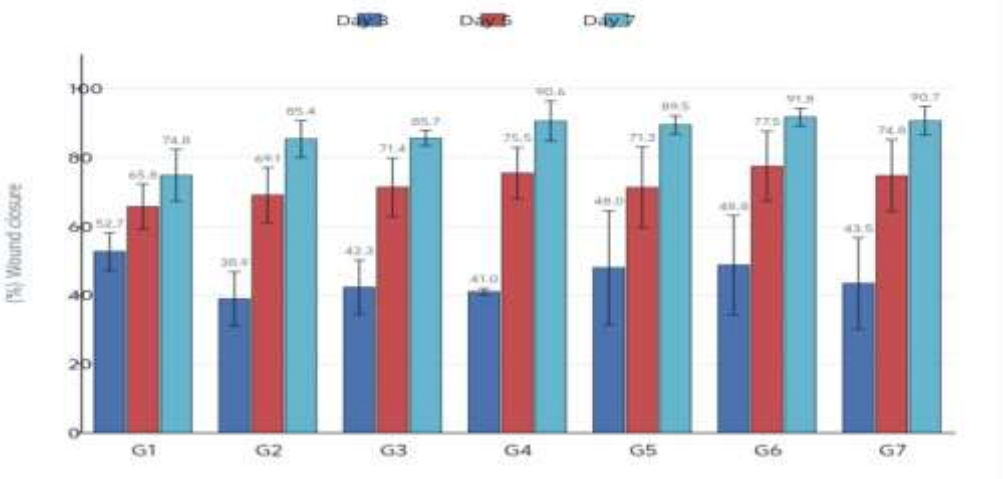


Figure 6. Mean percentage of wound closure onDay 3، 5، 7 in the control and treated groups.

The control groups (infected and treated with plain gel) showed lower closure (85.42% and 85.66%, respectively). However, the differences between the treated groups did not reach statistical significance (P>0.05). In contrast, Friedman's test showed that the effect of time was statistically significant(P<0.05), confirming the progression of wound healing over time across all groups.

For thermal imaging, the wound temperature gradually converged with that of healthy skin; the mean temperature gap ΔT decreased from -1.13°C on day 1 to -0.03°C on day 7. On day 7, the plant extract and plant nanoparticle groups recorded the smallest thermal gap (0.07 and 0.10 °C respectively), reflecting excellent thermal convergence, although there were no statistically significant differences in the amount of thermal normalization between the groups (P>0.05) (Table 5).

Table 5. Signed ΔT values for each group on Days 3, 4 and 7 (mean ± SD for available replicates).

Day	G1	G2	G3	G4	G5	G6	G7
Day 3	−0.50± 0.32	−0.57 ± 0.32	−0.35 ± 0.62	0.4± 0.56	−0.93 ± 0.67	−0.88 ± 0.40	−1.28 ± 0.19
Day 5	−0.43± 0.18	−0.40 ± 0.44	−0.30 ± 0.75	+0.35 ± 0.37	−0.60 ± 0.94	−0.33 ± 1.36	−0.55 ± 0.26
Day 7	+0.30± 0.08	−0.37 ± 0.06	−0.23 ± 0.23	+0.30 ± 0.35	+0.07 ± 0.06	+0.10 ± 0.10	−0.37 ± 0.47

3.5 Bacterial Cultures:

Mannitol salt agar cultures showed bacterial growth in all infected experimental groups from day 1 to day 6. However, after day 6, no detectable *S. aureus* growth was observed in the groups treated with chemical nanoparticles, plant extract, plant

nanoparticles, and clindamycin, while bacterial infection continued to grow in the two control groups (untreated infected and blank gel)

3.6 Photographic Documentation:

The macroscopic appearance of the wounds was documented across the different days as shown in figure 7 and serial thermal images showing thermal changes in the wounds across the evaluation days were recorded asrepresented in figure 8.

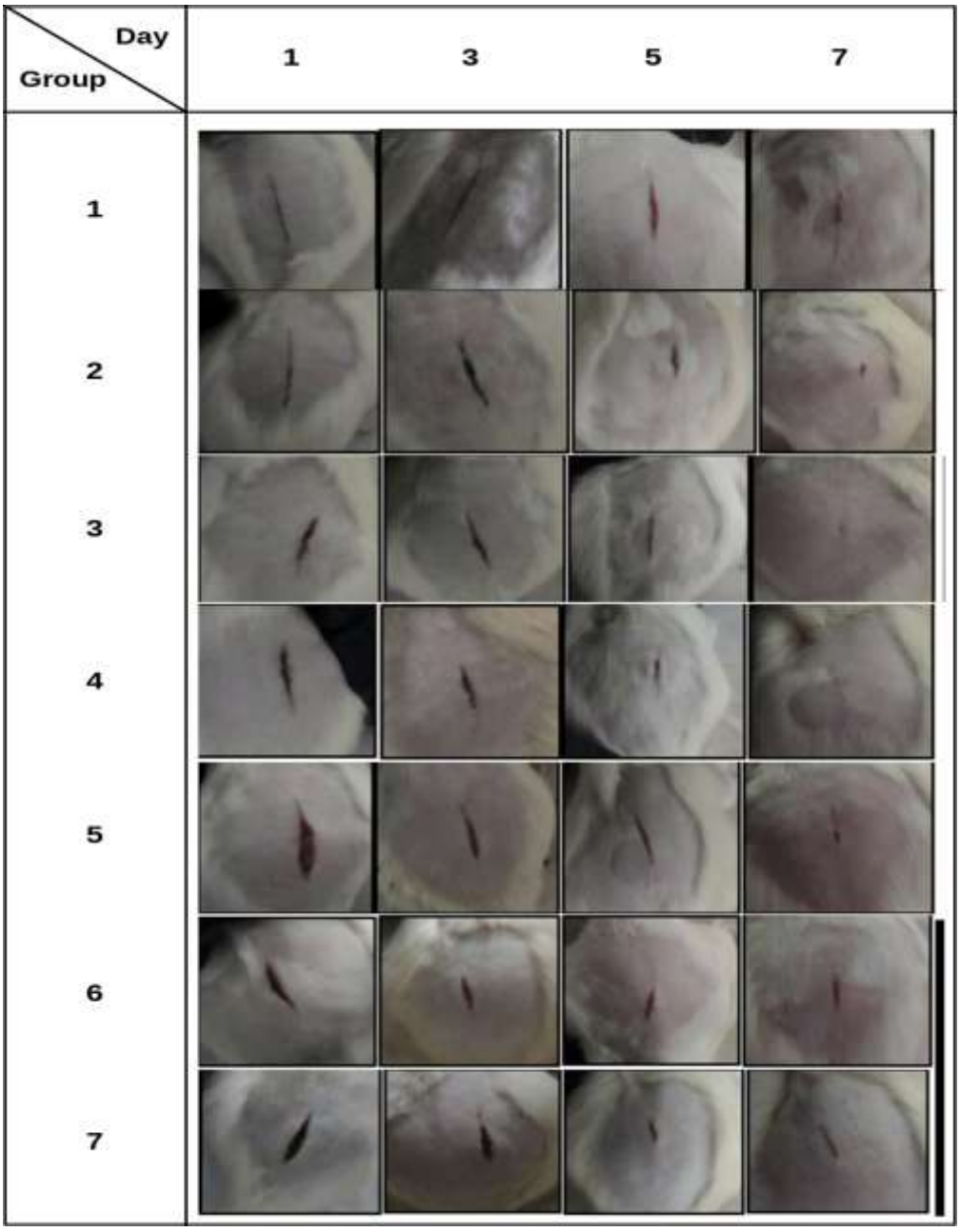


Figure 7. Photographs of the macroscopic wound appearance in the seven groups on Days 1, 3, 5, and 7.

Natural Resources for Human Health
eISSN: 2583-1194

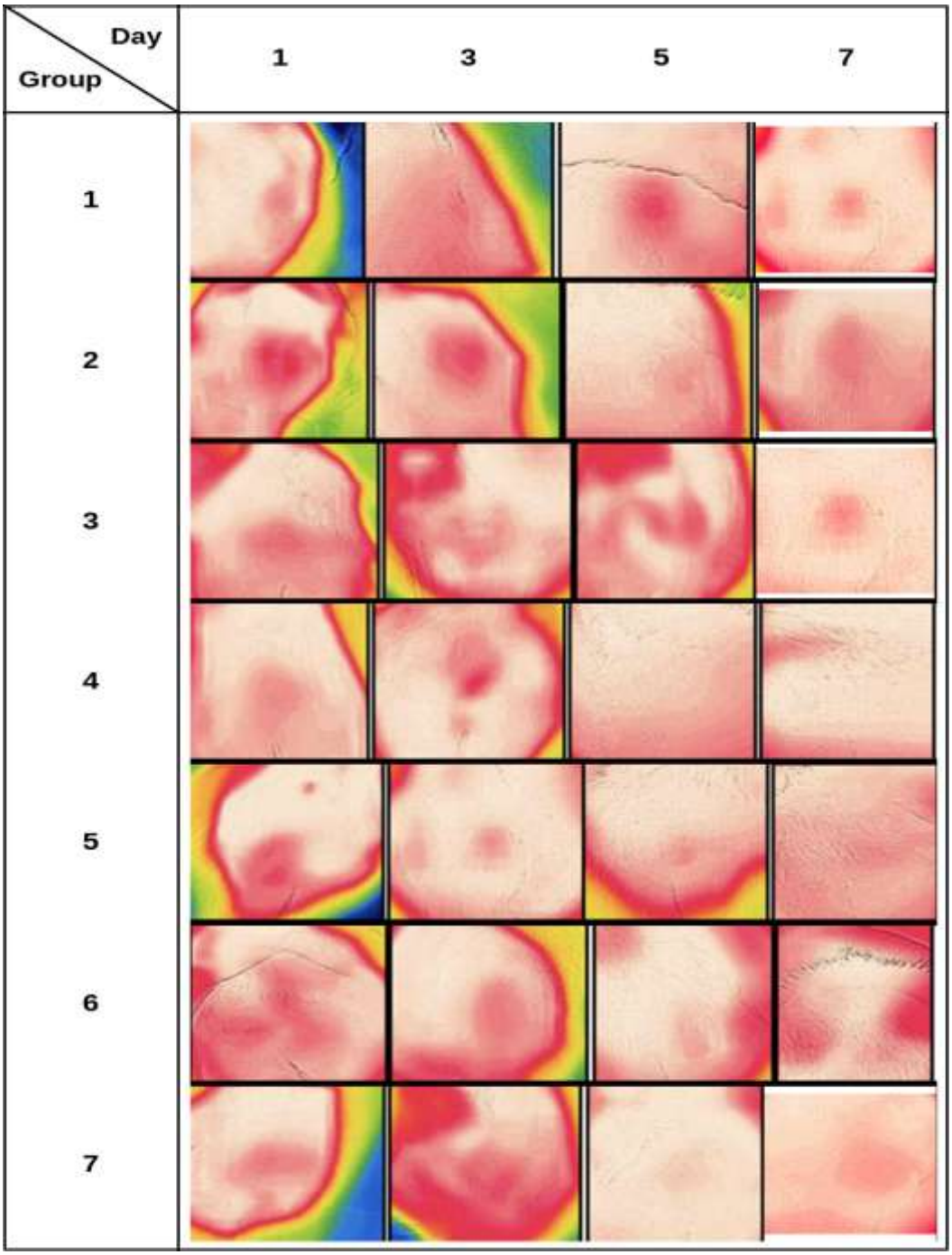


Figure 8. Serial infrared thermograms of wounds in the seven groups on Days 1, 3, 5, and 7.

4. DISCUSSION

The current work demonstrates that Hypericum perforatum plant extract, which is high in flavonoids and phenols, serves as a green reducing and capping agent. Asgharian and Ojani's phytochemical screening showed that leaves and flowers contain flavonoids and phenols, while the leaves contain coumarins and diterpenes, the extract also contains terpenoids, cardiac glycosides, and phlobatannins. However, our screening failed to find coumarin, which could be explained by regional and environmental variations [33]. This formation of nanoparticles was confirmed by the peaks in UV-Vis spectrum at (425, 440 nm) and the changes in the FTIR spectra, indicating the interaction between the plant biomolecules and the nanoparticle surface. These findings closely agreed with those reported by Alahmad et al. (2021) who observed UV absorbed ranging from

(392 to 460 nm), with a sharp peak at 442 nm [34]. Furthermore, the increase in the hydrodynamic diameter of the plant nanoparticles (114.33 nm) compared to the chemically synthesized ones (57.67 nm) is attributed to the organic coating (capping agent) composed of plant metabolites and PVP. Regarding the morphology, the observed in the scanning electron microscopy (SEM) images confirm the nanoparticles fail in nanometeric range with aggregation. The aggregation is likely a result of sample drying, the formation of polymeric films from PVP, or even colloidal aggregation induced by gold plating [35].

The superior antibacterial activity of plant mediated nanoparticles (P. NPs) compared to chemically synthesized nanoparticles despite their larger size and crude extracts may be related to a potential combined effect between silver ions and bioactive phenolic compounds bound to the particle surface. Although previous studied have reported stronger antibacterial activity for smaller AgNPs [36], surface-bound metabolites enhance overall particle-cell interaction. Alahmad et al. (2022) found MIC values for Hypericum perforatum mediated AgNPs of 6.25 µg/mL against Pseudomonas aeruginosa and 12.5 µg/mL against Staphylococcus aureus, all bacteria isolate was resistance to plant extract [10]. In comparison, our results found comperable MIC (20 µg/mL) for S. aureus and much higher MIC (200 µg/mL) for P. aeruginosa. unlike their finding, our plant extract showed antibacterial activity against both bacteria. However, E. coli was resistance to Hypericum perforatum mediated AgNPs in both researches. Notably, P. aeruginosa exhibited a discrepancy between the diffusion assay (large inhibition zones) and the microdilution assay (high MIC value). This reflects a difference in the diffusion mechanism across agar compared to direct exposure in liquid broth. The high tolerance of this Gram-negative bacterium is explained by intrinsic resistance mechanisms such as outer membrane permeability, efflux pumps, and biofilm formation [37].

The plant synthesized nanoparticles group (P. NPs) showed a superior therapeutic profile with the highest wound closure (91.80%), total bacterial clearance after day 6, and excellent thermal convergence (ΔT +0.10). On the other hand, the plant extract gel showed an initial lag in response followed by a strong healing advancement, reflecting the dual pharmacological role of phytoconstituents in promoting tissue repair and inhibiting microbiological development. These finding supported by Zain et al. (2024), who synthesized AgNPs using Dactyloctenium aegyptium and observed a wound contraction of 87.44 ± 4.12% on day 9 using an AgNP hydrogel, compared to 74.85 ± 2.92% with silver sulfadiazine and 65.51 ± 2.06% in untreated control animals [38]. Furthermore, infrared thermography proved to be an excellent non-invasive diagnostic tool for monitoring wound healing dynamics; the reduction in the thermal gap (ΔT) directly reflects microvascular recovery and tissue perfusion.. However, the untreated infected group showed partial thermal convergence and eventual closure despite persistent bacterial colonization. although complete wound closure will take longer period. This improvement can be attributed to host intrinsic immune defenses and natural regenerative capacity of the tissue [39].

The vehicle gel group (Carbopol) showed substantial wound closure (85.66%), suggesting that the gel base itself facilitate healing by maintaining a moist environment, reducing evaporative H2O loss, and protecting the wound surface, although lacking antibacterial action [40]. these results compared to those reported by Gaikwad et al. who found wound contraction of 87.01 ± 4.73% in gel treated group compared to 85.48 ± 15.99% in untreated group after 15 days [41]. In contrast, clindamycin achieved microbiological success and high closure, but its temperature on day 7 remained slightly negative (-0.37°C), suggesting that microbial clearance and wound closure may precede the full functional restoration of the surface temperature profile, possibly reflecting local perfusion differences [42].

5. CONCLUSION

The present study demonstrates that ethanolic extract of *Hypericum perforatum* can serve as effective and environmentally friendly reducing agent for green synthesis of silver nanoparticles. The plant-mediated nanoparticles exhibit greater antimicrobial efficacy than conventional chemical nanoparticles. This is due to the combined effect between the silver ions and the phenolic compounds of plants that encapsulate the particles. The incorporation of these green nanoparticles (P. NPs) in the Carbopol gel produced an acceptable topical formulation, skin pH compatibility and physicochemical characteristics. Further studies are required to confirm long-term safety optimize the formulation.

ACKNOWLEDGEMENTS

The authors would like to express their gratitude to the College of Pharmacy, University of Mosul, Mosul, Iraq, for providing the laboratory facilities and support necessary to conduct the experimental work of this research.

AUTHOR CONTRIBUTIONS

Maimonah Q. Yahya , Zena Sattam Hamad: Conceptualization, Investigation.

Abdulrhman A. Ismael , Maimonah Q. Yahya , Zena Sattam Hamad: Methodology, Laboratory Analysis.

Abdulrhman A. Ismael , Maimonah Q. Yahya , Zena Sattam Hamad: Data Curation, Formal Analysis.

Abdulrhman A. Ismael , Maimonah Q. Yahya , Zena Sattam Hamad: Supervision, Writing—Review&Editing.

CONFLICT OF INTEREST

The authors declare that there is no conflict of interest.

ETHICS STATEMENT

The experimental protocol for the animal wound-healing study was reviewed and approved by the Institutional Animal Ethical Committee (IAEC), College of Veterinary Medicine University of Mosul (approval no. UM.VET.2026.005).

DATA AVAILABILITY STATEMENT

All data and materials are available and can be submitted when needed.

REFERENCES

[1] Negut I, Grumezescu V, Grumezescu AM. Treatment strategies for infected wounds. Molecules. 2018 Sep 18;23(9):2392. https://doi.org/10.3390/molecules23092392 PMID:30231567; PMCID:PMC6225154.

[2] Abid KY, Yahya MQ. Antimicrobial and anti-oxidant activities of essential oils derived from some citrus peel. Military Medical Science Letters/Vojenské zdravotnické Listy. 2023 Jan 1;92(1):64. https://doi.org/10.31482/mmsl.2022.025

[3] Maghiar L, Maghiar PB, Pop O, Mitran AM, Muresan MM, Neamţu AA, et al. A comprehensive review of antimicrobial peptides and smart biomaterials in chronic wound therapy: overcoming biofilms, resistance, and translational barriers. Int J Mol Sci. 2026;27(13):5955. https://doi.org/10.3390/ijms27135955.

[4] Sabarudin NS, Ab Ghani N, Ahmat N, Harlin EW, Hao LQ, Handajani J, et al. Harnessing plant bioactive compounds in biomaterial scaffolds for advanced wound healing: a comprehensive review. Biomedicines. 2025;13(10):2414. https://doi.org/10.3390/biomedicines13102414.

[5] Haghighatpasand S, Moradi M, Moradi F, Shafiee F. Effect of *Hypericum perforatum* on early wound healing after tooth extraction: a randomized controlled clinical trial. Front Dent. 2026;23:8. https://doi.org/10.18502/fid.v23i8.21237.

[6] Călina IC, Scărişoreanu A, Demeter M, Mănăilă E, Crăciun G. Strategies for incorporating natural therapeutic agents into hydrogel dressings: innovations in wound healing. Polymers (Basel). 2025;17(23):3105. https://doi.org/10.3390/polym17233105.

[7] Yahya MQ, Khalil RR, Mohammed ET. Silver nanocomposites: a glimpse into their game-changing roles in antibacterial therapy. Journal of Faculty of Pharmacy of Ankara University. 2025;49(3):981-98. https://doi.org/10.33483/jfpau.1590697

[8] Karataş H, Eker F, Akdaşçi E, Bechelany M, Karav S. Silver nanoparticles in antibacterial research: mechanisms, applications, and emerging perspectives. Int J Mol Sci. 2026;27(2):927. https://doi.org/10.3390/ijms27020927.

[9] Madhusudanan M, Zhang J, Pandit S, Singh P, Jeong GJ, Khan F, et al. Green synthesis of silver nanoparticles: a review of polymer and antimicrobial drug combinations for enhanced antimicrobial applications. Adv NanoBiomed Res. 2025;5(12):2400194. https://doi.org/10.1002/anbr.202400194.

[10] Alahmad A, Al-Zereini WA, Hijazin TJ, Al-Madanat OY, Alghoraibi I, Al-Qaralleh O, et al. Green synthesis of silver nanoparticles using Hypericum perforatum L. aqueous extract with the evaluation of its antibacterial activity against clinical and food pathogens. Pharmaceutics. 2022;14(5):1104. https://doi.org/10.3390/pharmaceutics14051104.

[11] Asad NA, Erci F, Bayram F. Ratio-tuned green-synthesized Ag–Fe bimetallic nanoparticles embedded in electrospun gelatin/chitosan nanofibrous scaffolds for antibacterial applications. RSC Adv. 2026;16(28):25614-27. https://doi.org/10.1039/D6RA01562J.

[12] Ranatunga B, Sekar M, Hashmi AR, Zahra F, Ravi RN, Prashantha Kumar BR, et al. Biopolymer hydrogel-based nanocomposites functionalized with natural products for wound dressings: translational advances in drug design,

development, and therapeutic wound care. Drug Des Devel Ther. 2026;20:578261. https://doi.org/10.2147/DDDT.S578261.

[13] Kumar B, Jain V, Yadav DK, Dhua AK, Goel P, Jain D, et al. Heat for healing: a review of infrared thermography in medical diagnostics and therapy. J Med Phys. 2026;51(1):1-11. https://doi.org/10.4103/jmp.jmp_175_25.

[14] Firdouse S, Alam P. Phytochemical investigation of extract of Amorphophallus campanulatus tubers. Int J Phytomedicine [Internet]. 2011 [cited 2026 Sep 4];3(1):32-5. https://ijp.arjournals.org/index.php/ijp/article/view/75

[15] Kumar N, Upadhyay P, Saxena G. Phytochemical screening of pomegranate peel using crude hydro-alcoholic extract and pharmacological activities. J Sci Res Publications. 2018;8(1):193-9. https://www.ijsrp.org/research-paper-0118/ijsrp-p7326.pdf

[16] Jayaprakash A, Sangeetha R. Phytochemical screening of Punica granatum Linn. peel extracts. Journal of academia and industrial research. 2015 Oct;4(5):160-2. https://www.jairjp.com/OCTOBER%202015/04%20SANGEETHA.pdf

[17] Hossain MA, Al-Raqmi KAS, Al-Mijizy ZH, Weli AM, Al-Riyami Q. Study of total phenol, flavonoid contents and phytochemical screening of various leaf crude extracts of locally grown Thymus vulgaris. Asian Pac J Trop Biomed. 2013;3(9):705-10. https://doi.org//10.1016/S2221-1691(13)60142-2.

[18] Haider AJ, Abed AL, Ahmed DS. Formation silver nanoparticles of different size using different reductants with AgNO3 solution. Iraqi J Sci [Internet]. 2016 [cited 2026 Sep 4];57(2B):1203-9. https://ijs.uobaghdad.edu.iq/index.php/eijs/article/view/7342

[19] Baláž M, Balážová Ľ, Daneu N, Dutková E, Balážová M, Bujňáková Z, et al. Plant-mediated synthesis of silver nanoparticles and their stabilization by wet stirred media milling. Nanoscale Res Lett. 2017;12:83. https://doi.org/10.1186/s11671-017-1860-z.

[20] Sevinc-Sasmaz C, Erci F, Torlak E, Yöntem M. Characterization of silver nanoparticles synthesized using Hypericum perforatum L. and their effects on Staphylococcus aureus. Microsc Res Tech. 2025;88(8):2321-32. https://doi.org/10.1002/jemt.24862.

[21] Akintola AO, Kehinde BD, Ayoola PB, Adewoyin AG, Adedosu OT, Ajayi JF, et al. Antioxidant properties of silver nanoparticles biosynthesized from methanolic leaf extract of Blighia sapida. IOP Conf Ser Mater Sci Eng. 2020;805(1):012004. https://doi.org/10.1088/1757-899X/805/1/012004.

[22] Verma P, Maheshwari SK. Preparation of silver and selenium nanoparticles and its characterization by dynamic light scattering and scanning electron microscopy. J Microsc Ultrastruct. 2018;6(4):182-7. https://doi.org/10.4103/JMAU.JMAU_3_18.

[23] Yahya MQ, Abid KY. Evaluation of antimicrobial effects of citrus peel extracts and it's silver nanoparticles against multiple pathogens. Mil Med Sci Lett. 2022;91(3):244-55. https://doi.org/10.31482/mmsl.2021.052.

[24] Rodríguez-Melcón C, Alonso-Calleja C, García-Fernández C, Carballo J, Capita R. Minimum inhibitory concentration (MIC) and minimum bactericidal concentration (MBC) for twelve antimicrobials (biocides and antibiotics) in eight strains of Listeria monocytogenes. Biology (Basel). 2022;11(1):46. https://doi.org/10.3390/biology11010046.

[25] Gaikwad VL, Yadav VD, Dhavale RP, Choudhari PB, Jadhav SD. Effect of Carbopol 934 and 940 on fluconazole release from topical gel formulation: a factorial approach. J Curr Pharm Res. 2012;2(2):487-93 https://doi.org/10.33786/JCPR.2012.V02I02.004.

[26] Khan AW, Kotta S, Ansari SH, Sharma RK, Kumar A, Ali J. Formulation development, optimization and evaluation of aloe vera gel forwound healing. Pharmacogn Mag. 2013;9(Suppl 1):S6-10. https://doi.org/10.4103/0973-1296.117849.

[27] Dantas MGB, Reis SAGB, Damasceno CMD, Rolim LA, Rolim-Neto PJ, Carvalho FO, et al. Development and evaluation of stability of a gel formulation containing the monoterpene borneol. ScientificWorldJournal. 2016;2016:7394685. https://doi.org/10.1155/2016/7394685.

[28] Gujjar S, Madhavi BLR, Karki R. Formulation and evaluation of topical gel containing nanostructured lipid carrier dispersion of an antifungal drug. Acta Pharm Sci. 2019;57(4):57-75. https://doi.org/10.23893/1307-2080.APS.05724.

[29] Leanpolchareanchai J, Teeranachaideekul V. Topical microemulsions: skin irritation potential and anti-inflammatory effects of herbal substances. Pharmaceuticals (Basel). 2023;16(7):999. https://doi.org/10.3390/ph16070999.

[30] Tan WS, Arulselvan P, Ng SF, Mat Taib CN, Sarian MN, Fakurazi S. Improvement of diabetic wound healing by topical application of Vicenin-2 hydrocolloid film on Sprague Dawley rats. BMC Complement Altern Med. 2019;19:20. https://doi.org/10.1186/s12906- 018-2427-y

[31] Kant V, Gopal A, Kumar D, Gopalkrishnan A, Pathak NN, Kurade NP, et al. Topical pluronic F-127 gel application enhances cutaneous wound healing in rats. Acta Histochem. 2014;116(1):5-13. https://doi.org/10.1016/j.acthis.2013.04.010.

[32] Lin TS, Abd Latiff A, Abd Hamid NA, Wan Ngah WZ, Mazlan M. Evaluation of topical tocopherol cream on cutaneous wound healing in streptozotocin-induced diabetic rats. Evid Based Complement Alternat Med. 2012;2012:491027. https://doi.org/10.1155/2012/491027.

[33] Asgharian A, Ojani S. In vitro antioxidant activity and phytochemical screening of flowers and leaves of Hypericum perforatum L. ethanolic extracts from Tonekabon, Iran. J Phytochem Biochem. 2017;1(1):1-5.

[34] Alahmad A, Feldhoff A, Bigall NC, Rusch P, Scheper T, Walter JG. Hypericum perforatum L.-mediated green synthesis of silver nanoparticles exhibiting antioxidant and anticancer activities. Nanomaterials (Basel). 2021;11(2):487. https://doi.org/10.3390/nano11020487.

[35] Juhász L, Moldován K, Gurikov P, Liebner F, Fábián I, Kalmár J, et al. False morphology of aerogels caused by gold coating for SEM imaging. Polymers (Basel). 2021;13(4):588. https://doi.org/10.3390/polym13040588.

[36] Ali AY, Alani AK, Ahmed BO, Hamid LL. Effect of biosynthesized silver nanoparticle size on antibacterial and anti-biofilm activity against pathogenic multi-drug resistant bacteria. OpenNano. 2024;20:100213 https://doi.org/10.1016/j.onano.2024.100213

[37] Langendonk RF, Neill DR, Fothergill JL. The building blocks of antimicrobial resistance in Pseudomonas aeruginosa: implications for current resistance-breaking therapies. Front Cell Infect Microbiol. 2021;11:665759. https://doi.org/10.3389/fcimb.2021.665759.

[38] Zain M, Nayab S, Rashid Z, Aleem A, Raza H, Yousif MD. Biosynthesis and in vivo wound healing abilities of Dactyloctenium aegyptium-mediated silver nanoparticles used as hydrogel dressing. Process Biochem. 2024;147:31-8. https://doi.org/10.1016/j.procbio.2024.08.011.

[39] Cwajda-Białasik J, Mościcka P, Jawień A, Szewczyk MT. Infrared thermography to prognose the venous leg ulcer healing process: preliminary results of a 12-week, prospective observational study. Wound Repair Regen. 2020;28(2):224-33. https://doi.org/10.1111/wrr.12781.

[40] Nuutila K, Eriksson E. Moist wound healing with commonly available dressings. Adv Wound Care (New Rochelle). 2021;10(12):685-98. https://doi.org/10.1089/wound.2020.1232.

[41] Gaikwad S, Birla S, Ingle AP, Gade A, Ingle P, Golińska P, et al. Superior in vivo wound-healing activity of mycosynthesized silver nanogel on different wound models in rat. Front Microbiol. 2022;13:881404. d https://doi.org/10.3389/fmicb.2022.881404.

[42] Ramirez-GarciaLuna JL, Bartlett R, Arriaga-Caballero JE, Fraser RDJ, Saiko G. Infrared thermography in wound care, surgery, and sports medicine: a review. Front Physiol. 2022;13:838528. https://doi.org/10.3389/fphys.2022.838528.